

# Conjugated Polycyanines: A New Class of Materials with Large Third-Order Optical Nonlinearities

Zhong'an Li, Trenton R. Ensley, Honghua Hu, Yadong Zhang, Sei-Hum Jang, Seth R. Marder, David J. Hagan, Eric W. Van Stryland,\* and Alex K.-Y. Jen\*

All optical signal processing (AOSP) will be important components of future high-speed optical communications networks.<sup>[1]</sup> In AOSP, the propagation of a signal beam can be modulated by another beam of control light via an ultrafast third-order nonlinear optical (NLO) effect such as the optical Kerr effect, which gives rise to an irradiance-dependent refractive index,  $n(I) = n_0 + n_2 I$ , where  $n_0$  is the linear refractive index,  $I$  is the irradiance, and  $n_2$  is the nonlinear refractive index related to the real part of the third-order susceptibility ( $\text{Re}\chi^{(3)}$ ). Highly efficient AOSP materials require not only a large  $n_2$ , but also very low optical loss. For transparent materials, the primary loss is often due to two-photon absorption (2PA), denoted by the 2PA coefficient  $\alpha_2$ , which is an irradiance dependent loss related to the imaginary part of  $\chi^{(3)}$  ( $\text{Im}\chi^{(3)}$ ). Since an AOSP device requires the nonlinear phase shift to be much larger than the optical loss, it is useful to define a material figure-of-merit (FOM) as  $|\text{Re}\chi^{(3)}/\text{Im}\chi^{(3)}| = 4\pi n_2/\lambda_0 \alpha_2$  where  $\lambda_0$  is the vacuum wavelength.<sup>[1a]</sup> While 2PA is detrimental to AOSP, materials with large 2PA may be useful for other applications such as optical limiting,<sup>[2]</sup> microscopy,<sup>[3]</sup> and 3D microfabrication.<sup>[4]</sup>

In order to achieve large  $\text{Re}\chi^{(3)}$  for AOSP, much attention has been paid to develop new classes of organic third-order NLO chromophores.<sup>[5]</sup> In particular, interest in using symmetrical polymethine or cyanine dyes has increased rapidly due to their very large microscopic polarizabilities,  $\gamma (\propto \chi^{(3)}/N$ , where  $N$  is the number density of molecules), and favorable molecular FOM ( $|\text{Re}(\gamma)/\text{Im}(\gamma)|$ ) at optical telecommunication wavelengths (1.3 and 1.55  $\mu\text{m}$ ).<sup>[5,6]</sup> Cyanines have an odd-number of  $\text{sp}^2$ -hybridized carbon atoms along their planar and conjugated bridge bearing a highly delocalized charge, wherein the bond-length alternation (BLA) between adjacent C–C bonds is close to zero, giving rise to a maximal magnitude of  $\text{Re}(\gamma)$ , according

to the simplified perturbation theory.<sup>[7]</sup> As is well known, the extension of conjugation length ( $L$ ) of a cyanine will enhance the magnitude of  $\text{Re}(\gamma)$  dramatically (i.e.,  $\text{Re}(\gamma) \propto L^n$ ).<sup>[8]</sup> However, a Peierls-type symmetry breaking that localizes charge on one end of the molecule will occur if  $L$  is greater than nine  $\text{sp}^2$ -hybridized carbon atoms (C9), resulting in losing this favorable characteristic optical property of cyanines.<sup>[9]</sup>

One way to solve this problem is to modify the charge-stabilizing end groups of cyanines to enable more efficient delocalization of the  $\pi$ -electrons throughout the whole molecule, while still keeping  $L < \text{C9}$ .<sup>[6,10]</sup> For example, a heptamethine based on the selenopyrylium end group shows a very large  $\text{Re}(\gamma)$  of  $-2.2 \times 10^{-31}$  esu with a high molecular FOM, above 100 in dilute solutions.<sup>[6]</sup> However, only a few such cyanines are known to exist due to the synthetic difficulties involved, and thermo- and photo-chemical stabilities, and unfavorable aggregations between cyanines. Recently, polymethine dyes with large rigid groups bound to bridge and end groups were demonstrated to provide an effective mechanism to decrease chromophore–chromophore interactions as well as chromophore–counterion interactions. In this manner, material FOMs  $>12$  and reasonable low linear loss were realized.<sup>[11]</sup> However, an alternative approach is to design structures having symmetry persistent repeating cyanine units with shorter  $L$  that are fully conjugated with each other to form conjugated polycyanines. In such structures, the cyanine repeating units in the polymeric chains are connected via a “Janus core” (a conjugated bi-functional charge delocalizing group), which can provide extended delocalization pathways for the exciton beyond each individual cyanine unit along the polymeric chain of the polycyanine, according to the essential characteristics of excitons in conjugated polymers.<sup>[12]</sup> Furthermore, such a structural platform can be used to study electronic interactions and exciton delocalization between cyanines and polycyanine chains to potentially induce sizable enhancement of the nonlinearities, such as those observed in J-aggregated cyanines.<sup>[13]</sup> To date, fully conjugated polycyanines (PC1 and PC2, **Scheme 1**) have only been reported for photovoltaic applications, which showed significant bathochromic shifts ( $>150$  nm) in linear absorption relative to monomeric cyanines (C1 and C2) without causing detrimental symmetry breaking.<sup>[14]</sup>

To be useful for AOSP device applications, the cyanines need to be processed into optical quality thin films with high chromophore number density in order to have very large  $\chi^{(3)}$ .<sup>[5,15]</sup> Unfortunately, efficient translation from  $\gamma$  to  $\chi^{(3)}$  remains a major challenge in this field due to strong and random ion pairing and/or aggregation between ionic cyanines in the solid-state that often induce significant charge redistribution, electronic coupling, and distortion of the molecular

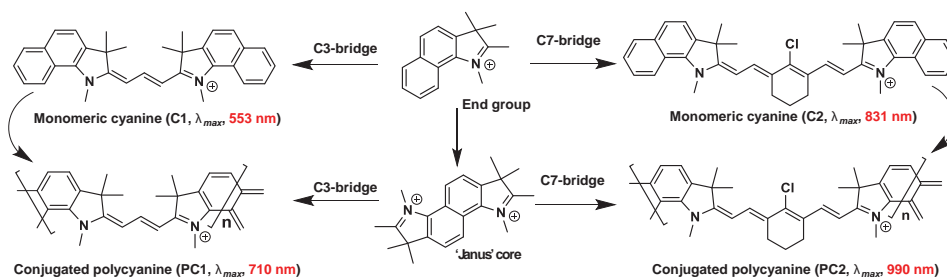
Dr. Z. Li, Dr. S.-H. Jang, Prof. A. K.-Y. Jen  
Department of Materials Science and Engineering  
University of Washington  
Seattle, WA 98195, USA  
E-mail: ajen@u.washington.edu

T. R. Ensley, Dr. H. Hu, Prof. D. J. Hagan,  
Prof. E. W. Van Stryland  
CREOL, The College of Optics and Photonics  
University of Central Florida  
Orlando, FL 32816, USA  
E-mail: ewvs@creol.ucf.edu

Dr. Y. Zhang, Prof. S. R. Marder  
School of Chemistry and Biochemistry and Center  
for Organic Photonics and Electronics  
Georgia Institute of Technology  
Atlanta, GA 30332-0400, USA



DOI: 10.1002/adom.201400631



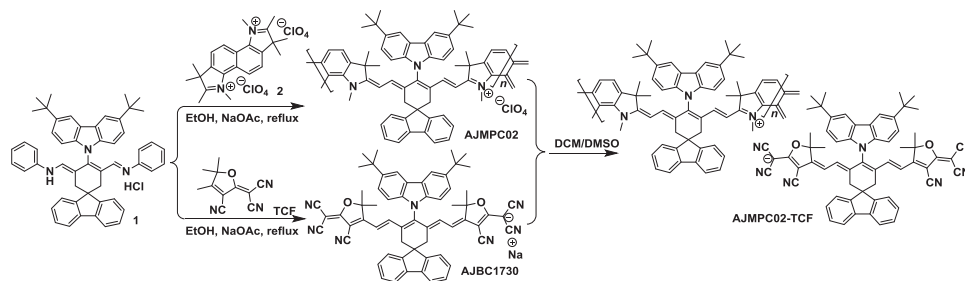
**Scheme 1.** The structure of the reported monomeric indolium cyanines and fully conjugated polycyanines.

symmetry leading to formation of undesirable 1- and 2-photon states.<sup>[16]</sup> In this regard, the fully conjugated polycyanines presented here could provide new structural mechanisms to address these issues in addition to potentially extending delocalization pathways beyond one cyanine unit. There are several unique structural merits of this material design such as, good optical properties of polycyanines can be readily achieved for device applications, in addition, polycyanines can be used as a polyelectrolyte to organize extended ionic structures or modulate aggregations through various self-assembly processes based on electrostatic interactions.<sup>[17]</sup> Indeed, both PC1 and PC2 (Scheme 1) do not show any asymmetric electronic transition peaks in the film absorption spectra relative to their monomeric cyanines C1 and C2.<sup>[14]</sup> Moreover, the cationic polycyanine can be used as a host polymer for anionic cyanines to form complementary polymeric cyanine complexes, wherein the anionic cyanines can function as mutually delocalized and polarizable counter ions for cationic cyanines and vice versa. In this way, the ion-pairing induced symmetry-breaking can be reduced while the concentration of active chromophores can be increased.

To realize all these advantages, we have developed a new indolium-based fully conjugated polycyanine (AJMPC02) and its corresponding polymeric cyanine complex (AJMPC02-TCF). In our design, a highly delocalized anionic heptamethine (AJBC1730) based on the 2-(3-cyano-4,5,5-trimethyl-5H-furan-2-ylidene)malononitrile (TCF) end group is selected as a counterion for AJMPC02 to form a polymeric cyanine salt complex. The TCF-heptamethines have been shown earlier to have large  $\chi^{(3)}$  values at 1.55  $\mu\text{m}$  that are three times larger than that of silicon.<sup>[15a]</sup> We have introduced two rigid and bulky substituents (carbazole and fluorene moieties) into the center of a seven

$\text{sp}^2$ -hybridized carbon atom (C7) based conjugation bridge for AJMPC02 and AJBC1730, which function as efficient spacers that possess an out of plane configuration of the chromophore  $\pi$ -system to prevent unwanted aggregation between polycyanine chains.<sup>[11]</sup> Considering that PC2 has been reported to possess rather poor solubility and processibility,<sup>[14]</sup> we have functionalized the spacers with solubilizing substituents (*tert*-butyl group) to improve solubility and processibility of the resulting polymers.

The synthetic route of making polycyanine and its salt complex is shown in **Scheme 2**. The C7-conjugating bridge **1** was synthesized as reported,<sup>[11]</sup> and the bifunctional “Janus core” of **2** was synthesized according to methods reported in the literature.<sup>[14]</sup> By refluxing in ethanol using sodium acetate as base, cationic polyindolinium of AJMPC02 and anionic TCF-cyanine of AJBC1730 could be prepared with good yields of 93.1% and 86.8%, respectively. Through a simple ion exchange, AJMPC02 was mixed with AJBC1730 to afford the desired salt complex of AJMPC02-TCF with 87.5% yield. Both the polycyanine and its salt complex have good solubility, and are readily soluble in common organic solvents such as dichloromethane (DCM) or dimethylformamide (DMF). Their <sup>1</sup>H NMR spectra are shown in Figures S1–S3, Supporting Information, and the data are consistent with their structures as shown in Scheme 2. The molecular weight and polydispersity ( $M_w/M_n$ , PDI) of AJMPC02 at different light scattering  $dn/dc$  values was confirmed by Gel Permeation Chromatography (GPC) using DMF containing 0.1 wt% LiBr as eluent, and the results are given in **Figure 1**. It was shown that the  $M_n$  value of AJMPC02 increased significantly at increasing polymer concentrations, and resulted in a large  $M_n$  value of  $1.56 \times 10^7$  at a  $dn/dc$  value of 0.022  $\text{mL g}^{-1}$ . This suggests that strong interactions exist between ionic



**Scheme 2.** Synthetic route to the polycyanine and its corresponding polymeric cyanine salt complex.

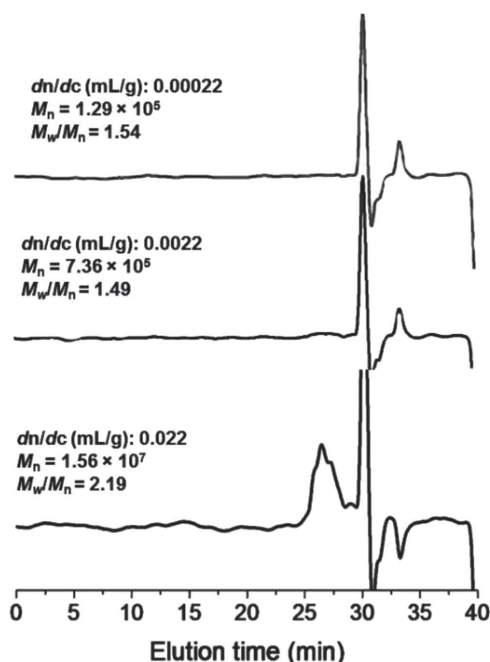


**Figure 1.** The GPC traces of AJMPC02 at different light scattering  $dn/dc$  values in DMF solutions.

polymeric chains of this polymer at high concentrations even with bulky substituents functionalized at the center of the conjugation bridge to prevent interchain interactions.

UV-vis-IR absorption spectra of these new polycyanines and monomeric TCF-cyanine in DCM solutions (concentration of  $\approx 2 \times 10^{-6}$  M) and as thin films ( $\approx 300$  nm thick) are shown in **Figure 2**, with the corresponding absorption maxima summarized in **Table 1**. Similar to PC2, AJMPC02 gives an absorption maximum at 1009 nm, a large bathochromic shift of 180 nm compared to that of monomeric cyanine C2, further suggesting the delocalization of the exciton can be extended over several cyanine units in the polymeric chain when going from monomeric cyanine to polycyanines.<sup>[14]</sup> Moreover, it should be noted that the absorption band of AJMPC02 retains the characteristics of highly polarizable and symmetric cyanines very nicely, with

**Table 1.** Linear optical properties of materials.

No.	$\lambda_{\max, \text{sol}}^{\text{a}}$ [nm]	$\lambda_{\max, \text{fil}}^{\text{a}}$ [nm]	$\epsilon_{\max}^{\text{b}}$ [ $10^5 \text{ M}^{-1} \text{ cm}^{-1}$ ]
AJMPC02	1009	960	1.5
AJBC1730	899	910	5.0
AJMPC02-TCF	900, 1003	930	1.6, 0.7

<sup>a</sup>) Absorption maxima wavelengths in dilute DCM solutions ( $\approx 2 \times 10^{-6}$  M) or in thin films ( $\approx 300$  nm); <sup>b</sup>) Molar extinction coefficients measured in dilute DCM solution. Error bars are estimated at  $\pm 2\%$ .

sharp transitions and very large extinction coefficients. This is one of the critical factors to realize large third-order optical nonlinearities.<sup>[5]</sup> After forming the polymeric cyanine complex, AJMPC02-TCF maintains the spectral features of both cationic AJMPC02 and anionic AJBC1730, with two identified absorption bands at 1003 and 900 nm, respectively. This indicates the negligible electronic interactions between these two complementary units in their ground-states.

In films, all absorption spectra (Figure 2B) exhibit increased band broadening compared to their corresponding solution spectra due to strong ion-pairing and/or aggregation in the solid state.<sup>[16]</sup> AJMPC02-TCF shows a much sharper absorption band edge and significantly reduced long-wavelength tail compared to AJMPC02, indicating somewhat alleviated ion-pairing and/or aggregation with the formed polymeric cyanine salt complex. This may help improve the optical quality of resulting films for AOSP device applications.<sup>[1a]</sup> However, AJMPC02 shows a  $\approx 50$  nm hypsochromic-shift in its film absorption maximum compared to that of the solution, possibly due to different kinds of aggregates formed by strong intermolecular interactions between ionic polymeric chains as suggested by the GPC measurements.

The 2PA and nonlinear refraction (NLR) coefficients of AJMPC02 and AJMPC02-TCF were measured in DCM solutions ( $1 \times 10^{-3}$  M) using the femtosecond pulsed dual-arm (DA) Z-scan technique at  $1.3 \mu\text{m}$ ,<sup>[18,19]</sup> and the results are summarized in **Table 2**. As opposed to the conventional Z-scan method,<sup>[18]</sup> the DA Z-scan allows subtraction of the background solution or substrate signal from the signal of interest, i.e., the

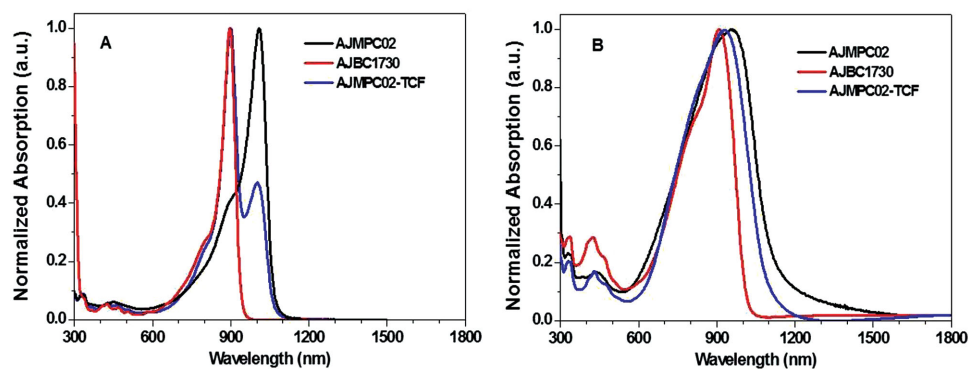


**Figure 2.** The absorption spectra in A) diluted DCM solutions and B) thin neat films (AJMPC02 and AJMPC02-TCF), and guest-host polycarbonate film doped with 50 wt% of AJBC1730.

**Table 2.** The third-order microscopic nonlinearities measured in concentrated DCM solutions using the femtosecond pulsed dual-arm Z-scan method at 1.3  $\mu\text{m}$ . The unit conversion from mks to esu can follow Equation (5).

No.	$\text{Re}(\gamma)$ [ $10^{-32}$ esu]	$\text{Im}(\gamma)$ [ $10^{-32}$ esu]	$ \gamma ^{(a)}$ [ $10^{-32}$ esu]	$ \text{Re}(\gamma)/\text{Im}(\gamma) $
AJMPC02	-7.3	6.0	9.4	1.2
AJMPC02-TCF	-4.5	1.8	4.8	2.7
Indo-C7-H <sup>b)</sup>	-1.0	0.59	1.2	1.7
AJBC1722 <sup>c)</sup>	-1.3	0.15	1.3	7.8
DOB-C9 <sup>d)</sup>	-5.7	0.79	5.7	7.2

<sup>a)</sup> $|\gamma| = [\text{Re}(\gamma)^2 + \text{Im}(\gamma)^2]^{1/2}$ ; <sup>b)</sup>From ref. [21]; <sup>c)</sup>From ref. [15a]; <sup>d)</sup>From ref. [8a].

solute or thin film. As explained in the Supporting Information, this technique greatly increases the signal-to-noise ratio.

To relate the measured  $n_2$  and  $a_2$  to  $\chi^{(3)}$  and  $\gamma$ , we use the following relations

$$\alpha_2^{\text{mks}} = \frac{3\omega \text{Im}\chi_{\text{mks}}^{(3)}}{2\epsilon_0 c^2 n_0^2} \quad (1)$$

$$n_2^{\text{mks}} = \frac{3\text{Re}\chi_{\text{mks}}^{(3)}}{4\epsilon_0 c n_0^2} \quad (2)$$

where  $\omega$  is the angular frequency defined as  $2\pi c/\lambda_0$  with  $c$  being the speed of light, and  $\epsilon_0$  is the vacuum permittivity. All universal constants are in mks units, i.e., m, kg, s. The conversion from  $\chi^{(3)}$  to  $\gamma$  is as follows

$$\chi_{\text{mks}}^{(3)} = \epsilon_0^{-1} N f^{(3)} \gamma_{\text{mks}} \quad (3)$$

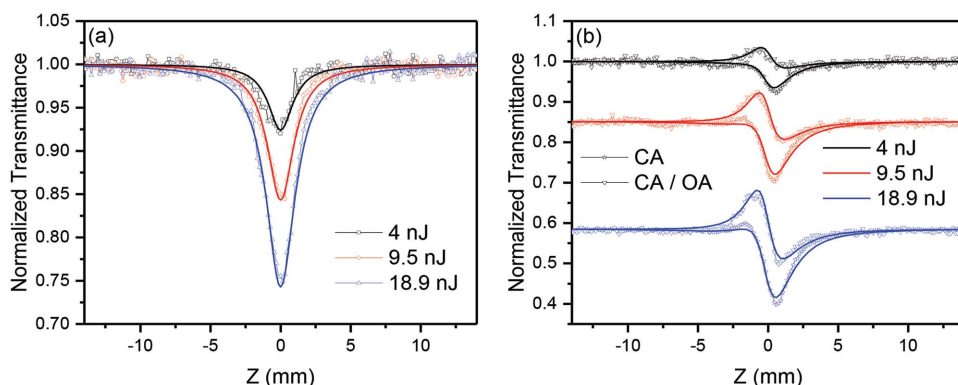
with the third-order local field correction  $f^{(3)} = ((n_0^2 + 2)/3)^4$ . The conversion from mks to esu follows as

$$\chi_{\text{mks}}^{(3)} = \frac{4\pi}{9} \times 10^{-8} \chi_{\text{esu}}^{(3)} \quad (4)$$

$$\gamma_{\text{esu}} = 9 \times 10^{14} (4\pi\epsilon_0)^{-1} \gamma_{\text{mks}} \quad (5)$$

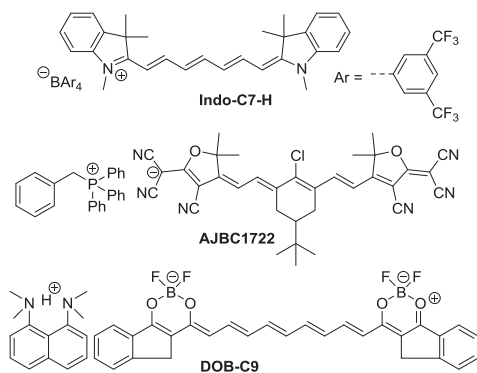
where the units in mks are  $\text{m}^2 \text{V}^{-2}$  for  $\chi^{(3)}$  and  $\text{C m}^4 \text{V}^{-3}$  for  $\gamma$ , while the units in esu are  $\text{cm}^2 \text{statvolt}^{-2}$  for  $\chi^{(3)}$  and  $\text{cm}^5 \text{statvolt}^{-2}$  for  $\gamma$ .

Figure 3 presents DA Z-scans of a  $1 \times 10^{-3}$  M DCM solution of AJMPC02 with both open aperture (OA) and closed aperture (CA) signals to determine  $a_2$  and  $n_2$ , respectively. Using the aforementioned relations, we then calculate  $\text{Im}(\gamma)$  and  $\text{Re}(\gamma)$  based upon  $a_2$  and  $n_2$  following Equations (1)–(3). From Figure 3a, the OA Z-scan signals from all three pulse energy measurements are fit with  $\alpha_2 = 0.22 \pm 0.04 \text{ cm GW}^{-1}$  corresponding to  $\text{Im}(\gamma) = 6.0 \pm 1.5 \times 10^{-32} \text{ esu}$  ( $7.4 \pm 1.9 \times 10^{-57} \text{ mks}$ ). In the case of CA Z-scans, both NLR and 2PA are present, thus the 2PA coefficient obtained from the OA scans was held fixed allowing a one-parameter fit to ascertain the effective value of  $n_2$ . Dividing the CA Z-scan signal by the OA signal gives the results shown in Figure 3b that look like pure NLR signals. The effective values of  $n_2$  obtained from the CA Z-scans were  $-(3.2 \pm 1.0) \times 10^{-15} \text{ cm}^2 \text{W}^{-1}$ ,  $-(4.3 \pm 0.86) \times 10^{-15} \text{ cm}^2 \text{W}^{-1}$ , and  $-(5.3 \pm 1.1) \times 10^{-15} \text{ cm}^2 \text{W}^{-1}$  for pulsed excitations of 4 nJ, 9.5 nJ, and 18.9 nJ, respectively. This change in  $n_2$  with respect to irradiance is indicative of excited state refraction (ESR) where free carriers created by 2PA change the index of refraction. At low irradiance,  $n_2$  dominates the change in index whereas at higher irradiance the effects of ESR add a higher order nonlinear refraction signal.<sup>[20]</sup> Thus, the contribution from the pure Kerr nonlinearity is given in the limit of zero irradiance. To ascertain this value, a linear regression fit to the data gives the slope, related to the ESR cross-section, and the zero-crossing, which yields the bound-electronic  $n_2$ . Extrapolating the aforementioned values to zero irradiance yields  $n_2 = -(2.8 \pm 0.56) \times 10^{-15} \text{ cm}^2 \text{W}^{-1}$ , corresponding to  $\text{Re}(\gamma) = -(7.3 \pm 1.8) \times 10^{-32} \text{ esu}$  ( $-(9.0 \pm 2.3) \times 10^{-57} \text{ mks}$ ). We note here that the magnitude of  $\gamma$  values (Table 2) of AJMPC02 represents one of the largest values ever reported, which are much greater than those observed in most indolium<sup>[21]</sup> or TCF-based<sup>[15a]</sup> monomeric cyanines with the same conjugation length (C7) such as Indo-C7-H and AJBC1722 (Scheme 3), and even larger than that of DOB-C9 (Scheme 3),<sup>[8a]</sup> which has a longer conjugation length C9. This confirms our hypothesis that connecting cyanine molecules into fully conjugated polycyanines significantly enhances molecular third-order optical



**Figure 3.** a) Open-aperture (OA) dual-arm (DA) Z-scans of a  $1 \times 10^{-3}$  M solution of AJMPC02 in DCM and b) closed-aperture (CA) DA Z-scans along with the divided result of the CA signal by the OA signal with three different pulse energy measurements at a wavelength of 1.3  $\mu\text{m}$ . The solid lines in a) and b) are the fits to the data using the usual Z-scan theory.<sup>[18]</sup>





**Scheme 3.** The structure of Indo-C7-H, AJBC1722, and DOB-C9.

nonlinearities without increasing the conjugation bridge length, but via an extended delocalization of the exciton over several cyanine units in the polycyanine. However,  $\text{Im}(\gamma)$  is also dramatically increased which gives a relatively low FOM of 1.2. This may be caused by the electronic coupling between cyanine molecules in the polycyanine allowing the transition of the low-lying 2-photon states to be close to the one-photon state.<sup>[16a]</sup>

Somewhat unexpectedly, exchanging the counterions of AJMPC02 from  $\text{ClO}_4^-$  to anionic TCF-cyanines results in a decrease of both  $\text{Re}(\gamma)$  and  $\text{Im}(\gamma)$  for AJMPC02-TCF (Table 2), although the concentration of active chromophores has been increased. This may be attributed to the relative concentration of the polycyanine chain in AJMPC02-TCF, which is decreased compared to that in AJMPC02 when using the large TCF-cyanine as counterions, since polycyanine makes a larger contribution to nonlinearities than the one from the counterionic TCF-cyanine as shown in Table 2. Nonetheless, such an ion exchange approach could be quite useful in terms of providing additional flexibility in material design. It has been demonstrated that the Coulombic interaction between a cationic cyanine and anionic counterion is a major driving force to the symmetry-breaking that can significantly alter the mean BLA, and subsequent NLO properties of polymethines.<sup>[16a]</sup> In particular, small, strongly polarizing counterions such as  $\text{ClO}_4^-$  have a more pronounced ion-pairing induced symmetry-breaking effect.<sup>[16c]</sup> Indeed, the resulting salt complex AJMPC02-TCF shows a decreased  $\text{Im}(\gamma)$  compared to  $\text{Re}(\gamma)$  that improves the FOM to 2.7, likely due to the mitigation of deleterious ion-pairing effects by using delocalized cyanines as counterions.

To understand the efficacy of translating between the molecular third-order nonlinear properties of polycyanines to bulk properties, thick neat films (870 nm) of AJMPC02-TCF were prepared and measured by the DA Z-scan method at both

1.3 and 1.55  $\mu\text{m}$ , and the nonlinear parameters are summarized in Table 3. Figure 4a shows OA DA Z-scans at different pulse energies to determine  $\alpha_2$ . All OA Z-scans can be fit with  $\alpha_2 = 90 \pm 18 \text{ cm GW}^{-1}$ . The refractive index of 1.98 at 1.3  $\mu\text{m}$  was determined via prism coupling which leads to the calculation of  $\text{Im}\chi^{(3)} = 9.4 \pm 1.9 \times 10^{-11} \text{ esu}$  ( $1.3 \pm 0.26 \times 10^{-18} \text{ mks}$ ). Assuming a film density of  $1.1 \text{ g cm}^{-3}$  and a dopant concentration of 100% leads to a determination of the number density, which allows us to calculate  $\text{Im}(\gamma) = 1.7 \pm 0.43 \times 10^{-32} \text{ esu}$  ( $2.1 \pm 0.42 \times 10^{-57} \text{ mks}$ ). All CA DA Z-scans, as shown in Figure 4b, can be fit with the same  $n_2 = -(1500 \pm 300) \times 10^{-15} \text{ cm}^2 \text{ W}^{-1}$  indicative of no ESR processes which corresponds to  $\text{Re}\chi^{(3)} = -(15 \pm 3) \times 10^{-11} \text{ esu}$  ( $-(2.1 \pm 0.42) \times 10^{-18} \text{ mks}$ ) and  $\text{Re}(\gamma) = -(2.7 \pm 0.68) \times 10^{-32} \text{ esu}$  ( $-(3.3 \pm 0.66) \times 10^{-57} \text{ mks}$ ) using the refractive index and assumed number density. Moreover, the refractive index at 1.55  $\mu\text{m}$  is measured to be 1.89, thus the  $\text{Re}\chi^{(3)}$  and  $\text{Im}\chi^{(3)}$  at 1.55  $\mu\text{m}$  were found to be  $-(6.1 \pm 1.2) \times 10^{-11} \text{ esu}$  and  $9.4 \pm 1.9 \times 10^{-11} \text{ esu}$ , respectively, as shown in Table 3.

It is worth noting that the  $\gamma$  values extrapolated from  $\chi^{(3)}$  values of these neat films at 1.3  $\mu\text{m}$  (Table 3) are in reasonable agreement with the values determined from the solutions (Table 2), suggesting an excellent translation between  $\gamma$  and  $\chi^{(3)}$ , namely, that the chromophores in polycyanine salt complexes can retain their cyanine-like characteristics well after being processed into high number density solid films. Furthermore, as shown in Table 4, the  $\text{Re}\chi^{(3)}$  values for these neat films at both 1.3 and 1.55  $\mu\text{m}$  are much larger than those of other well-known inorganic materials that are commonly used in the telecom windows.<sup>[22–24]</sup> Besides, these values compare favorably with most reported organic third-order materials in this spectral window including highly polarizable cyanines such as TCF-<sup>[15a]</sup> and thiopyrylium-<sup>[11,16b]</sup> heptamethine dyes ( $\approx 5 \times 10^{-11} \text{ esu}$ ). Similar to solution results, however, it is also accompanied by a relatively poor FOM of 1.5 and 0.7 at 1.3 and 1.55  $\mu\text{m}$ , respectively, due to appreciable 2PA loss. However, it is of note that the measured values of  $\alpha_2$  for the neat AJMPC02-TCF film are significantly larger than those found in semiconductors in this wavelength range. For example, these values are 3.3 and 9.6 times larger than those of GaAs at 1.3  $\mu\text{m}$  ( $\alpha_2 = 27 \pm 5 \text{ cm GW}^{-1}$ )<sup>[24]</sup> and 1.55  $\mu\text{m}$  ( $\alpha_2 = 7.8 \pm 2 \text{ cm GW}^{-1}$ )<sup>[25]</sup> respectively. Thus, this new molecular design may present a new manner in which to fabricate materials of interest for applications where large 2PA is desired.<sup>[2–4,26]</sup>

In conclusion, we have prepared a new cyanine-based fully conjugated polymer, AJMPC02, using a simple bifunctional indolium group as a “Janus core” to react with a bulky substituent functionalized C7-conjugating bridge. Moreover, its corresponding complementary salt complex with anionic TCF

**Table 3.** The macroscopic third-order susceptibility of AJMPC02-TCF measured in neat films using the femtosecond pulsed dual-arm Z-scan method at 1.3 and 1.55  $\mu\text{m}$ . The unit conversion from mks to esu can follow Equation (5).

Wavelength [ $\mu\text{m}$ ]	$n_2$ [ $10^{-15} \text{ cm}^2 \text{ W}^{-1}$ ]	$\text{Re}\chi^{(3)}$ [ $10^{-11} \text{ esu}$ ]	$\alpha_2$ [ $\text{cm GW}^{-1}$ ]	$\text{Im}\chi^{(3)}$ [ $10^{-11} \text{ esu}$ ]	$ \chi^{(3)} ^a$ [ $10^{-11} \text{ esu}$ ]	$ \text{Re}\chi^{(3)}/\text{Im}\chi^{(3)} $	Cal. $\text{Re}(\gamma)^b$ [ $10^{-32} \text{ esu}$ ]	Cal. $\text{Im}(\gamma)^b$ [ $10^{-32} \text{ esu}$ ]
1.3	-1500	-15.0	90	9.4	17.7	1.5	-2.7	1.7
1.55	-600	-6.1	75	9.4	11.2	0.7	-1.1	1.7

<sup>a</sup>)  $|\chi^{(3)}| = [(\text{Re}\chi^{(3)})^2 + (\text{Im}\chi^{(3)})^2]^{1/2}$ ; <sup>b</sup>) Extrapolated neat values were determined using Equations (1)–(5), where the values of  $\chi^{(3)}$  were taken from Table 3.

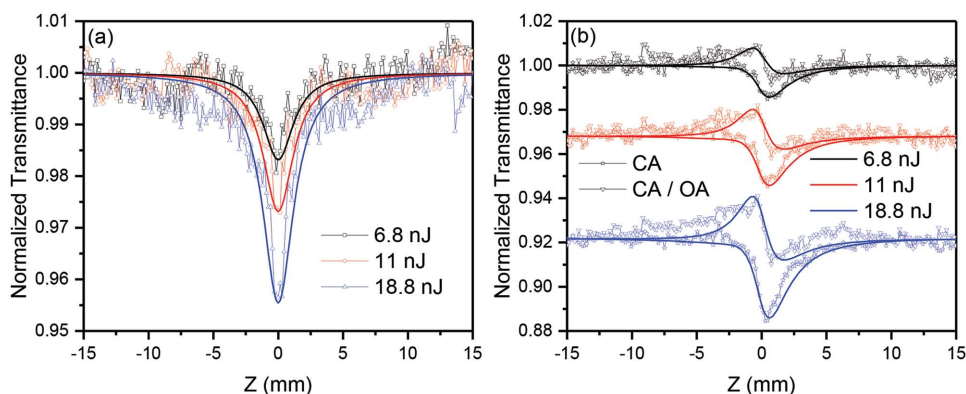


**Figure 4.** a) OA DA Z-scans of an 870 nm thick AJMPC02-TCF neat film using three different pulse energies and b) CA DA Z-scans along with the divided result of the CA signal by the OA signal with three different pulse energy measurements at a wavelength of 1.3  $\mu\text{m}$ . The solid lines in a) and b) are the fits to the data using the usual Z-scan theory.<sup>[18]</sup>

**Table 4.** The Comparison of  $|\text{Re}\chi^{(3)}|$  values in various materials.

No.	$ \text{Re}\chi^{(3)} $ [ $10^{-11}$ esu]	1300 nm	1550 nm
GaAs <sup>a)</sup>	0.59		2.9
Silicon [110] <sup>b)</sup>	0.81		1.3
As <sub>2</sub> Se <sub>3</sub> <sup>c)</sup>	N/A		1.1
AJMPC02-TCF	15		6.1

<sup>a)</sup>Values obtained and measured by Z-scan technique with bulk sample by CREOL authors; <sup>b)</sup>From ref. [22], and actual measurements taken at 1274 nm and 1540 nm; <sup>c)</sup>From ref. [23].

heptamethines as a counterion, AJMPC02-TCF, was also synthesized to mitigate the deleterious ion-pairing effect. The third-order optical nonlinearities of the two polycyanine salts were investigated in detail via an accurate and sensitive Dual-Arm Z-scan technique. The microscopic  $\text{Re}(\gamma)$  value of AJMPC02 was found to be as large as  $-7.3 \times 10^{-32}$  esu ( $-9.0 \times 10^{-57}$  mks) at 1.3  $\mu\text{m}$ , which is comparable to the best molecular AOSP material reported. This indicates that a sizable enhancement of  $\gamma$  for a cyanine can be achieved without increasing the length of the conjugating bridge, but through extending the delocalization of the exciton over several cyanine units in fully conjugated polycyanines. More encouragingly, the salt complex of AJMPC02-TCF exhibits very good processibility for device applications, and its neat films show one of the highest magnitudes of  $\text{Re}\chi^{(3)}$ ,  $-1.5 \times 10^{-10}$  esu ( $-2.1 \times 10^{-18}$  mks) measured at 1.3  $\mu\text{m}$ , suggesting the polycyanine is an efficient material system to translate large  $\gamma$  into large  $\chi^{(3)}$  in films for AOSP applications. Future work will be focused on optimizing the structure of the polycyanine to reduce two-photon loss while maintaining a large nonlinear refractive index.

## Supporting Information

Supporting Information is available from the Wiley Online Library or from the author.

## Acknowledgements

This work was supported by grants from the AFOSR MURI (FA9550-10-1-0558). Alex K.-Y. Jen thanks the Boeing-Johnson Foundation for its

support. CREOL researchers also acknowledge NSF MRI 1229563 and ECS 1202471 for funding. We thank Dr. Hua Wei for GPC measurements.

Received: December 21, 2014  
Revised: February 2, 2015  
Published online: February 26, 2015

- [1] a) J. Leuthold, C. Koos, W. Freude, *Nat. Photon.* **2010**, *4*, 535; b) K. Nozaki, T. Tanabe, A. Shinya, S. Matsuo, T. Sato, H. Taniyama, M. Notomi, *Nat. Photon.* **2010**, *4*, 477; c) M. Hochberg, T. Baehr-Jones, G. Wang, M. Shearn, K. Harvar, J. Luo, B. Chen, Z. Shi, R. Lawson, P. Sullivan, A. K.-Y. Jen, L. Dalton, A. Scherer, *Nat. Mater.* **2006**, *5*, 703.
- [2] L. W. Tutt, T. F. Boggess, *Prog. Quant. Electron.* **1993**, *17*, 299.
- [3] F. Helmchen, W. Denk, *Nat. Methods* **2005**, *2*, 932.
- [4] a) S. Maruo, O. Nakamura, S. Kawata, *Opt. Lett.* **1997**, *22*, 132; b) K. D. Belfield, K. J. Schafer, Y. Liu, J. Liu, X. Ren, E. W. Van Stryland, *J. Phys. Org. Chem.* **2000**, *13*, 837.
- [5] J. M. Hales, S. Barlow, H. Kim, S. Mukhopadhyay, J.-L. Brédas, J. W. Perry, S. R. Marder, *Chem. Mater.* **2013**, *26*, 549.
- [6] J. M. Hales, J. Matichak, S. Barlow, S. Ohira, K. Yesudas, J.-L. Brédas, J. W. Perry, S. R. Marder, *Science* **2010**, *327*, 1485.
- [7] a) R. L. Gieseking, S. Mukhopadhyay, C. Risko, S. R. Marder, J.-L. Brédas, *Adv. Mater.* **2014**, *26*, 68; b) D. Lu, G. Chen, J. W. Perry, W. A. Goddard III, *J. Am. Chem. Soc.* **1994**, *116*, 10679; c) S. R. Marder, C. B. Gorman, F. Meyers, J. W. Perry, G. Bourhill, J. L. Brédas, B. M. Pierce, *Science* **1994**, *265*, 632.
- [8] a) J. M. Hales, S. Zheng, S. Barlow, S. R. Marder, J. W. Perry, *J. Am. Chem. Soc.* **2006**, *128*, 11362; b) T. Johr, W. Werncke, M. Pfeiffer, A. Lau, L. Dähne, *Chem. Phys. Lett.* **1995**, *246*, 521.
- [9] a) L. M. Tolbert, X. Zhao, *J. Am. Chem. Soc.* **1997**, *119*, 3253; b) H. Hu, O. V. Przhonska, F. Terenziani, A. Painelli, D. Fishman, T. R. Ensley, M. Reichert, S. Webster, J. L. Bricks, A. D. Kachkovski, D. J. Hagan, E. W. Van Stryland, *Phys. Chem. Chem. Phys.* **2013**, *15*, 7666.
- [10] a) H.-C. Lin, H. Kim, S. Barlow, J. M. Hales, J. W. Perry, S. R. Marder, *Chem. Commun.* **2011**, *47*, 782; b) J. D. Matichak, J. M. Hales, S. Ohira, S. Barlow, S. H. Jang, A. K.-Y. Jen, J. L. Brédas, J. W. Perry, S. R. Marder, *ChemPhysChem* **2010**, *11*, 130.
- [11] S. Barlow, J.-L. Brédas, Y. A. Gemanenko, R. L. Gieseking, J. M. Hales, H. Kim, S. R. Marder, J. W. Perry, C. Risko, Y. Zhang, *Mater. Horiz.* **2014**, *1*, 577.
- [12] a) J.-L. Brédas, D. Beljonne, V. Coropceanu, J. Cornil, *Chem. Rev.* **2004**, *104*, 4971; b) G. D. Scholes, G. Rumbles, *Nat. Mater.* **2006**, *5*, 683.

- [13] a) A. Einfeld, J. S. Briggs, *Chem. Phys.* **2002**, *28*, 61; b) V. V. Shelkovich, F. A. Zhuravlev, N. A. Orlova, A. I. Plekhanov, V. P. Safonov, *J. Mater. Chem.* **1995**, *5*, 1331; c) K. Kemnitz, K. Yoshihara, T. Tani, *J. Phys. Chem.* **1990**, *94*, 3099; d) Y. Wang, *J. Opt. Soc. Am. B* **1991**, *8*, 981.
- [14] T. Geiger, H. Benmansour, B. Fan, R. Hany, F. Nüesch, *Macro. Rapid. Commun.* **2008**, *29*, 651.
- [15] a) Z. Li, Y. Liu, H. Kim, J. M. Hales, S.-H. Jang, J. Luo, T. Baehr-Jones, M. Hochberg, S. R. Marder, J. W. Perry, A. K.-Y. Jen, *Adv. Mater.* **2012**, *24*, OP326; b) C. Koos, P. Vorreau, T. Vallaitis, P. Dumon, W. Bogaerts, R. Baets, B. Esembeson, I. Biaggio, T. Michinobu, F. Diederich, W. Freude, J. Leuthold, *Nat. Photon.* **2009**, *3*, 216.
- [16] a) S. Mukhopadhyay, C. Risko, S. R. Marder, J. L. Brédas, *Chem. Sci.* **2012**, *3*, 3103; b) A. Scarpaci, A. Nantalaksakul, J. M. Hales, J. D. Matichak, S. Barlow, M. Rumi, J. W. Perry, S. R. Marder, *Chem. Mater.* **2012**, *24*, 1606; c) P.-A. Bouit, C. Aronica, L. Toupet, B. L. Guenic, C. Andraud, O. Maury, *J. Am. Chem. Soc.* **2010**, *132*, 4328.
- [17] A. Ciferri, *Chem. Eur. J.* **2010**, *16*, 10930.
- [18] M. Sheik-Bahae, A. Said, T.-H. Wei, D. J. Hagan, E. W. Van Stryland, *IEEE J. Quant. Electron.* **1990**, *26*, 760.
- [19] M. R. Ferdinandus, M. Reichert, T. R. Ensley, H. Hu, D. A. Fishman, S. Webster, D. J. Hagan, E. W. Van Stryland, *Opt. Mater. Express* **2012**, *2*, 1776.
- [20] A. A. Said, M. Sheik-Bahae, D. J. Hagan, T. H. Wei, J. Wang, J. Young, E. W. Van Stryland, *J. Opt. Soc. Am. B* **1992**, *9*, 405.
- [21] J. D. Matichak, J. M. Hales, S. Barlow, J. W. Perry, S. R. Marder, *J. Phys. Chem. A* **2011**, *115*, 2160.
- [22] M. Dinu, F. Quochi, H. Garcia, *Appl. Phys. Lett.* **2003**, *82*, 2954.
- [23] S. Shabahang, G. Tao, M. P. Marquez, H. Hu, T. R. Ensley, P. J. Delfyett, A. F. Abouraddy, *J. Opt. Soc. Am.* **2014**, *31*, 450.
- [24] W. C. Hurlbut, Y.-S. Lee, K. L. Vodopyanov, P. S. Kuo, M. M. Fejer, *Opt. Lett.* **2007**, *32*, 668.
- [25] The value of GaAs at 1.55  $\mu\text{m}$  was obtained and measured by Z-scan technique with bulk sample by CREOL authors.
- [26] a) P. Hrobárik, V. Hrobáriková, V. Semak, P. Kasák, E. Rakovský, I. Polyzos, M. Fakis, P. Persephonis, *Org. Lett.* **2014**, *16*, 6358; b) Y. M. Poronik, V. Hugues, M. Blanchard-Desce, D. T. Gryko, *Chem. Eur. J.* **2012**, *18*, 9258; c) P. Hrobárik, V. Hrobáriková, I. Sigmundová, P. Zahradník, M. Fakis, I. Polyzos, P. Persephonis, *J. Org. Chem.* **2011**, *76*, 8726.